https://doi.org/10.18321/ectj885

# Investigation of Gold Electrosorption onto Gold and Carbon Electrodes using an Electrochemical Quartz Crystal Microbalance

**Z. Mansurov[1,3]*, Zh. Supiyeva[1,3], Kh. Avchukir[2,3], A. Taurbekov[1,3], M. Yeleuov[1], G. Smagulova[1,3], M. Mansurova[3], M. Biisenbayev[1], V. Pavlenko[1,3]**

[1]Institute of Combustion Problems, 172, Bogenbai Batyr str., Almaty, Kazakhstan
[2]Center of Physical Chemical Methods of Research and Analysis, 96a, Tole bi str., Almaty, Kazakhstan
[3]al-Farabi Kazakh National University, 71, al-Farabi ave., Almaty, Kazakhstan

**Article info**

*Received:*
17 March 2019

*Received in revised form:*
26 June 2019

*Accepted:*
6 August 2019

**Keywords**
Gold
Activated carbon,
Rice husk,
Electrochemical quartz crystal microbalance

**Abstract**

The adsorption behavior of $Au^{3+}$ ions on metal electrodes has been studied using an electrochemical quartz crystal microbalance combined with the cyclic voltammetry technique. The experiments were carried out for $HAuCl_4$ using 0.1 mol·L$^{-1}$ HCl (pH~1) as a background electrolyte solution. The kinetics of electroreduction of $Au^{3+}$ ions on the rice husk based activated carbon and gold electrodes in chloride electrolytes by the cyclic voltammetry and the electrochemical quartz crystal microbalance with a variation of the scan rate in the range of 5–50 mV·s$^{-1}$ has been studied. The diffusion coefficient of $Au^{3+}$ ions for the tested solution on gold and carbon electrodes was determined by the cyclic voltammetry method on the basis of the Randles-Ševčik equation. It is found that electroreduction of gold goes via the discharge of $AuCl_4^-$ complexes to the formation of metallic gold with a current efficiency of 97–99%. The scanning electron microscopic images of the gold adsorbed carbon surface was taken to see gold particles and their morphology. In SEM images, it is clearly seen that the surface of carbon has a relief structure and gold has grown in the form of clusters. The smallest gold nanoparticles that could be examined were 100–250 nm in diameter on the surface of the carbon electrode.

## 1. Introduction

The electrochemical quartz crystal microbalance (EQCM) is a modern powerful method used in electrochemical experiments. EQCM monitors the change of frequency simultaneously with the electrochemical signal. The change in frequency is associated with changes in mass due to deposition or adsorption of a substance or dissolution of a substance from a working electrode [1].

The EQCM has been used simultaneously with quasi-steady state techniques like cyclic voltammetry (CV). Mass changes during electrolysis can be determined from A/(AmM) vs. potential curves, while A/(AmM) vs. charge density curves allow evaluating the number of Faraday exchanged per mole of electro-active species using Faraday's law of electrolysis. The change in the frequency of oscillation ($\Delta f$) is sensitive to the change in mass deposited on the crystal surface ($\Delta$m), thus meaning that any variation in the mass of the electrode will proportionally change the frequency at which the crystal oscillates [2]. The relationship between $\Delta f$ and $\Delta$m is given by the Sauerbrey [3] Eq. (1):

$$\Delta f = -Cf \cdot \Delta m \quad (1)$$

where $\Delta f$ is the change in frequency (Hz), $C_f$ is the sensitivity factor of the crystal (0.0815 Hz·ng$^{-1}$·cm$^{-2}$ for a 6 MHz at 20 °C) and $\Delta$m is the change in mass per unit area (g·cm$^{-2}$).

$C_f$ is provided by Eq. (2), shown above, in which $n$ is the number of harmonic at which the crystal is driven (this factor is set to 1, by design), $f$ is the resonant frequency of the fundamental mode of the loaded crystal (Hz), $\rho_q$ is the density of quartz (2.648 g·cm$^{-3}$) and $\mu_q$ is the shear modulus of quartz (2.947·10$^{11}$ g·cm$^{-1}$·s$^{-2}$).

$$Cf = \frac{2n \cdot f^2}{\sqrt{\rho_q \cdot \mu_q}} \quad (2)$$

*Corresponding author. E-mail: zmansurov@kaznu.kz

From Eqs. (1) and (2), the change in mass can be calculated as follows (Eq. 3):

$$\Delta m = -\frac{\Delta f}{Cf} \quad (3)$$

In [4], the authors compared the response of EQCM during the very early stages of the deposition of silver and copper on a gold substrate. Formation of copper ions as soluble intermediates during the deposition of copper causes a deviation of the frequency response from the expected one theoretically. Significant stress, which is observed only in the case of copper, is attributed to a large difference in the lattice parameter between gold and copper. During silver deposition, the frequency response follows the Sauerbrey equation, and no stress is observed.

The authors of [5–6] applied EQCM method when investigating copper electrodeposition. Anodic oxidation of copper electrodes in alkaline solutions was investigated using EQCM, CV, chronoamperometry (CA) and electrochemical impedance spectroscopy (EIS) measurements [5]. The participation of $Cu^{3+}$ soluble species in the electrocatalytic oxidation of ethanol was proved by EQCM measurements, these data providing valuable information on the mechanism of the electrode process and formation of $Cu^{2+}$ insoluble species from the reaction of $Cu^{3+}$ with ethanol. Also, the results on the copper electrodeposition mechanism at different pH values were obtained using EQCM [6]. Direct reduction of $Cu^{2+}$ and copper oxide (CuO) reduction at pH 2.0 and 4.5 occur simultaneously.

Activated carbon is a carbon-containing adsorbent having a large surface area and a developed porous structure. Activated carbon can be obtained from carbon-containing raw materials (rice husk, apricot stones, walnut shells, etc.) by physical and chemical activation methods [7–10]. According to the literature review, there are many works on using carbon adsorbents for adsorption of metals ($Au^{3+}$, $Cr^{6+}$, $As^{3+}$ and others) and metal compounds [11–17]. However, only a few publications on the use of EQCM method for the study of $Au^{3+}$ ions on the activated carbon adsorbents can be found in the literature.

In this study, we focused on the electrochemical quartz crystal microbalance method. This article reports on a study of $Au^{3+}$ ions adsorption on activated carbon and gold electrodes for comparison by a combined electrochemical quartz crystal microbalance-cyclic voltammetry (EQCM-CV) method. The frequency change during the adsorption of $Au^{3+}$ ions was determined by EQCM simultaneously measuring the electrical charge in the electrochemical experiments.

## 2. Experimental

The resonant frequency of quartz crystal and electrochemical experiments were monitored by Autolab Potentiostat/Galvanostat Model AUT83945 (PGSTAT302N). The detection of chloroauric solution ($HAuCl_4$) was carried out by EQCM-CV analysis. The EQCM-CV studies were conducted in a three electrode cell with quartz plate coated with activated carbon and gold electrode the active surface of which was 0.361 $cm^2$, gold wire (Au) as a counter electrode, and saturated Ag/AgCl in 3 $mol \cdot L^{-1}$ KCl as a reference electrode. A working solution with the concentration of 100 $mg \cdot L^{-1}$ was prepared by diluting the contents of the ampoules of the state standard sample of $Au^{3+}$ ions (company «IRGIREDMET», Russia) with distilled water. The basic background electrolyte was a solution of 0.1 $mol \cdot L^{-1}$ hydrochloric acid.

The working electrode was made by coating a quartz plate with activated carbon from rice husk. Carbon coating consists of 85 wt.% activated carbon, 10 wt.% polyvinylidene fluoride (PVDF) from Sigma-Aldrich and 5 wt.% carbon black (C-65, Timcal C-NERGY Imerys). A detailed description of the procedure for producing activated carbon is given in [18]. The morphology of activated carbon after sorption of gold ions was determined by scanning electron microscopy (SEM, Quanta 3D 200i Dual System, FEI). The surface area of activated carbon was investigated on the analyzer «Sorbtometr M» by low-temperature nitrogen adsorption using the method of Brunauer-Emmett-Teller (BET-method). As shown previously [18], the obtained carbon material from rice husk has a specific surface area of 2900 $m^2 \cdot g^{-1}$.

## 3. Results and Discussion

### *3.1. Electroreduction of Gold on a Gold Electrode*

The carbonized and activated rice husk (CARH) has a rather low redox potential and the stationary potential is 0.05 V (Ag/AgCl). The measured stationary (real) potential of [$AuCl_4^-$] in a hydrochloric acid medium is equal to 0.47 V (Ag/AgCl). The potential difference between gold (oxidizing agent) and the sorbent (reducing agent) is 0.42 V relative to the reference.

Figure 1a shows the cyclic voltammetry measurements and the frequency variation using the EQCM-CV procedure. These curves correspond to the deposition of $Au^{3+}$ ions on a gold-coated quartz crystal electrode, in 100 mg·L$^{-1}$ $HAuCl_4$ during a potential scan between 0 and 0.95 V at a scan rate of 5 mV·s$^{-1}$. Scanning starts from + 0.8 V to the cathode region. All frequency changes were measured with respect to the zero ΔFrequency which was set using the Reset EQCM ΔFrequency command while the working electrode was kept at 0.95 V vs Ag/AgCl (3 M KCl).

As the potential is scanned in the positive direction, the mass deposition of $Au^{3+}$ ions onto gold-electrode starts at around +0.65 V. This is followed by a sharp increase of cathodic current at around +0.5 V, which is detected by a sharp decrease in EQCM ΔFrequency. The frequency continues to decrease after the lower vertex potential is reached until the current passes through 0 and becomes positive again. This triggers an increase of the frequency and the ΔFrequency value finally returns to roughly 0 Hz at the positive end of the scan as the deposited gold is removed from the surface.

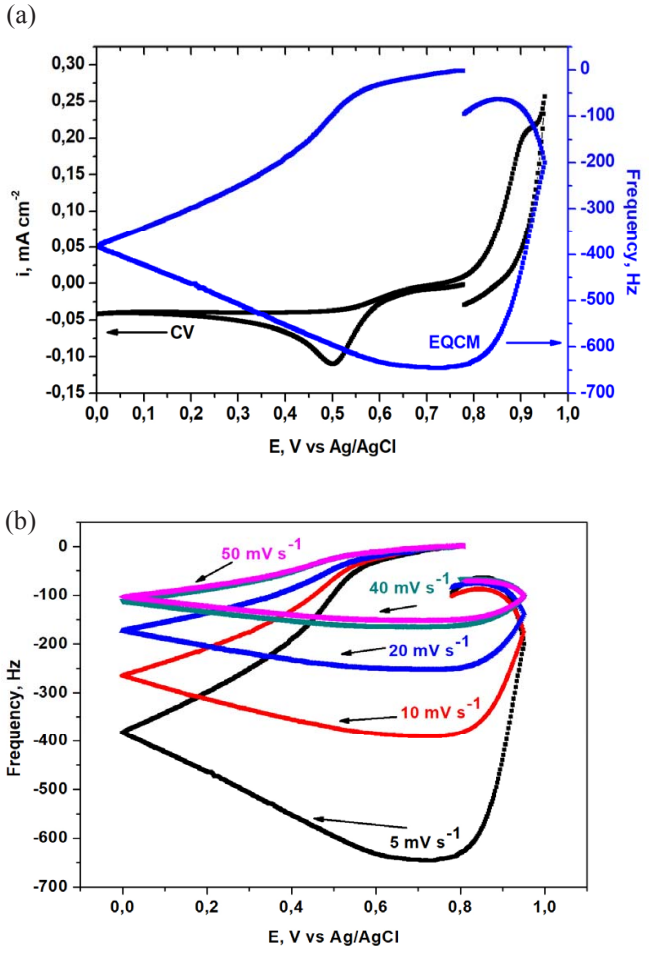


Fig. 1. (a) – Cyclic voltammetry and ΔFrequency vs. potential plots recorded with gold electrode in 100 mg·L$^{-1}$ $HAuCl_4$ solution at 5 mV·s$^{-1}$, (b) – Frequency plots for a gold electrode at various scan rates: 5, 10, 20, 40 and 50 mV·s$^{-1}$.

Figure 1b illustrates the changes in the mass of the electrode during the discharge-ionization process of a gold electrode on a piezoelectric element within the cell filled with a gold-containing acidic solution. The figure shows the minima of the change in the frequency of the oscillation of the piezoelectric quartz. If we take the absolute values then the maxima are seen. The change in the value of the oscillation frequency is given with a negative sign because during the electrodeposition of gold, an increase in the mass of the element occurs, thus leading to a decrease in the oscillation frequency. Prior to the start of voltammetric measurements, a calibration was carried out to take into account the influence of the solution mass on the change in frequency of the oscillation of the piezoelectric quartz, while the point zero (start of measurement) corresponds to the open circuit potential $E_{ocp}$.

A further decrease in the oscillation frequency from a potential of -0.8 to 0 V can be divided into two sections. The first section to -0.4 V, which is nonlinear, corresponds to the formation of the effective thickness of the diffusion layer and is characterized by a peak on the curve of the voltammogram. The second section has a linear shape during which the electroreduction of gold at a limiting diffusion current is observed at -0.4 ... 0 V ... -0.6 V (the diffusion layer has an effective thickness). The observed minima of the oscillation frequency of the piezoelectric crystal characterize the mass of electrodeposited gold, in particular, at a potential scan rate of 5 mV·s$^{-1}$, the minimum oscillation frequency is 645.82 Hz.

By integrating the I – t curve of the measured voltammograms, the amount of electricity (Q) spent on the reduction of gold was calculated and presented in Table 1. From the value of $\Delta f$, the practical mass ($m_{pr}$) of gold after its electrodeposition was calculated according to Eq. 1.

Since the practical mass was known, then according to Faraday's law it was possible to calculate the number of electrons participating in the reaction. As shown in Table 1, the calculated values of the number of electrons are equal to three; this allows us to represent the electroreduction of gold according to the following reaction:

$$AuCl_4^- + 3e = Au^0 + 4Cl^- \quad (4)$$

**Table 1**
Comparison of the theoretical value ($\Delta m_{Au}^{th}$) with the practical one ($\Delta m_{Au}^{pr}$) for gold electrode

| Electrode | Scan rate, mV·s$^{-1}$ | Q, 10$^{-3}$ C | -$\Delta f$, Hz | $m_{pr}$, 10$^{-6}$ g | $m_{th}$, 10$^{-6}$ g | CE, % | n |
|---|---|---|---|---|---|---|---|
| Gold | 5 | 4.28 | 645.82 | 2.86 | 2.91 | 98.28 | 2.98 |
| | 10 | 2.53 | 388.41 | 1.73 | 1.83 | 99.83 | 2.99 |
| | 20 | 1.68 | 250.71 | 1.11 | 1.14 | 97.36 | 2.97 |
| | 40 | 1.03 | 158.31 | 0.70 | 0.70 | 99.85 | 2.99 |
| | 50 | 9.57 | 146.79 | 0.65 | 0.65 | 99.84 | 2.99 |

Based on the known number of electrons, the current efficiencies (CE) of the gold electrodeposition process were calculated and presented below.

When the potential stepped from 0.95 V (a value where no Au is deposited on the gold electrode surface) to +0.7 V, the average change in frequency was measured as being 645.82 Hz. Using Sauerbrey's Eq. (1), the change in frequency can be correlated to the change in mass. Comparing the theoretical value ($\Delta m_{Au}^{th}$) with the experimental one ($\Delta m_{Au}^{exp}$), a very good agreement can be seen (Table 1).

The recorded cyclic voltammetry for gold electrodes at different scanning rates from 5 mV·s$^{-1}$ to 50 mV·s$^{-1}$ is shown in Fig. 2. The inserted plot shows the dependence of the peak of the cathodic current on the square root of the scan rate.

It is seen in the figure that an increase in the cathode current ($j_{pc}$) coincides with an increase in the potential scan rate (v). This dependence is described by the Randles- Ševčik equation, while the linear dependence $j_{pc}$ vs. v$^{1/2}$ (Fig. 2) indicates the diffusion limitation of this process. From the slope of the linear dependence, the diffusion coefficient of ions $AuCl_4^-$ in the solution was calculated to be equal to 1.6·10$^{-5}$ cm$^2$·s$^{-1}$.

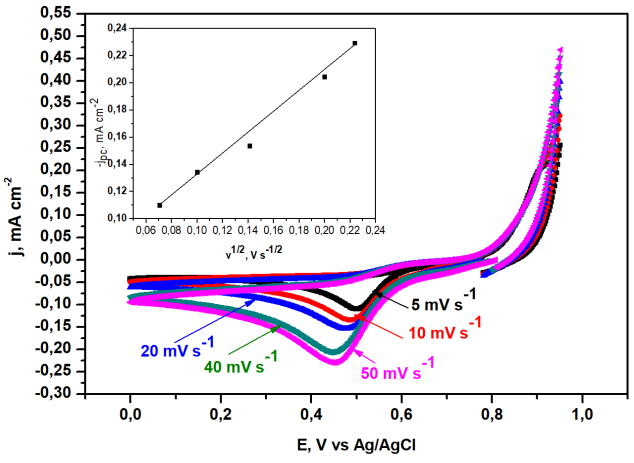


Fig. 2. Cyclic voltammograms for a gold quartz-crystal in 100 mg·L$^{-1}$ $HAuCl_4$ solution of various scan rates: 5, 10, 20, 40 and 50 mV·s$^{-1}$.

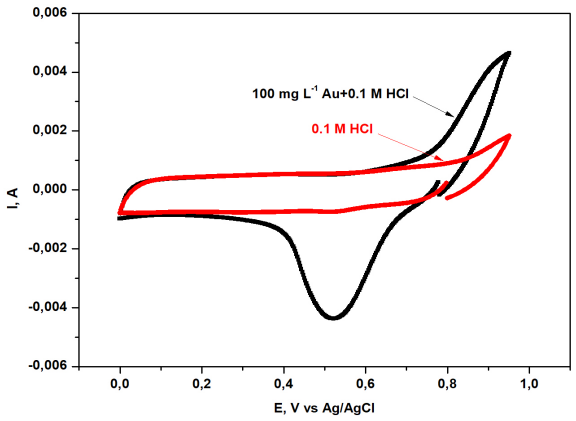


Fig. 3. Cyclic voltammograms on carbon electrode in black curve – 0.1 M HCl + 100 mg·L$^{-1}$ $HAuCl_4$ and red curve – 0.1 M HCl at 5 mV· s$^{-1}$.

### *3.2. Electroreduction of gold on a carbon electrode*

Cyclic voltammetry was performed on carbon-capped electrodes, and as can be seen in Fig. 3 (black curve) this resulted in an oxidative peak (0.80 V) in the reverse scan and a reductive peak (0.55 V) in the forward scan. In the background electrolyte 0.1 M HCl, a carbon electrode was also examined in this potential region (Fig. 3, red curve). However, no clear redox processes were observed. Since CARH has a large surface area, large charge-discharge currents of the double electric layer (non-Faraday currents) were revealed on the voltammogram. Thereby in order to calculate the kinetic data on the gold electroreduction reaction on this material, compensation should be made for a non-Faraday current.

For this purpose, the currents of a double electric layer (Fig. 3, red curve) were taken from the value of the cathodic current peak (Fig. 3, black curve). Finally, the resulting peak current values – $j_{pc}$ were used to calculate the diffusion coefficient. Figure 4a illustrates cyclic voltammograms of the background electrolyte, which were used subsequently to compensate for non-Faraday currents.

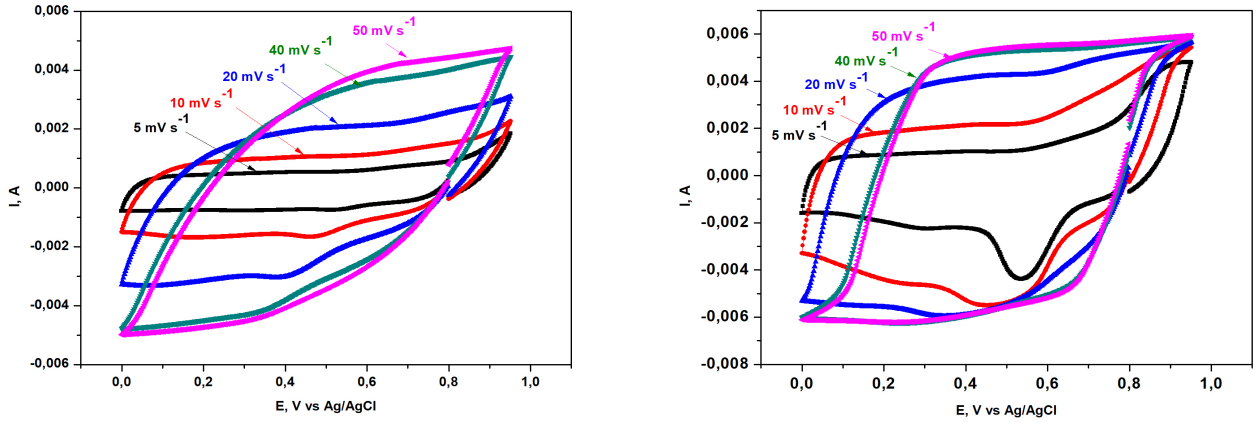


(a) (b)

Fig. 4. Cyclic voltammograms on carbon electrode in (a) 0.1 M HCl and (b) 0.1 M HCL + 100 mg·L$^{-1}$ $HAuCl_4$ of various scan rates: 5, 10, 20, 40 and 50 mV·s$^{-1}$.

Figure 4b demonstrates cyclic voltammograms of a gold-containing electrolyte and visible cathodic current peaks. However, at relatively high potential scan rates (20–50 mV·s$^{-1}$), cathode current peaks are not observed, thus indicating a high surface area of the carbon electrode that does not have time to be fully charged during short measurement times. In this regard, to detect current peaks ($j_{pc}$), low potential scan rates of 1 mV·s$^{-1}$ to 10 mV·s$^{-1}$ were selected. As can be seen in Fig. 5, at low electrode polarization rates, cathodic current peaks are clearly visible.

The presence of cathodic current peaks will make it possible to determine the kinetic parameters of the reaction in case if the compensation of charge-discharge currents of the electric double-layer is correct. The linear dependence $j_{pc}$ vs. $v^{1/2}$ (Fig. 5 Inset) was also determined from the voltammograms of the carbon electrode and the diffusion coefficient of $Au^{3+}$ ions was equal to 56.0 cm$^2$·s$^{-1}$·g$^{-1}$. The increased value of the diffusion coefficient of gold ions during the electroreduction of $AuCl_4^-$ – ions on the carbon electrode is four orders of magnitude higher than that on the gold electrode.

The overestimated value of the diffusion coefficient in this case (in aqueous electrolytes, the diffusion coefficient of ions varies in the region of $10^{-3}$ cm$^2$ s$^{-1}$ ÷ $10^{-7}$ cm$^2$·s$^{-1}$) is explained by the high specific surface of the activated electrode and the calculated apparent diffusion coefficients need to be adjusted for the mass of the carbon material. In addition, the voltammogram (Fig. 5) shows that the potential difference ($\Delta E_p$) of the anode ($E_{pa}$) and the cathode peak ($E_{pc}$) is approximately 60 mV less than that of the gold electrode and the cathode currents are ~ 50 times higher, respectively.

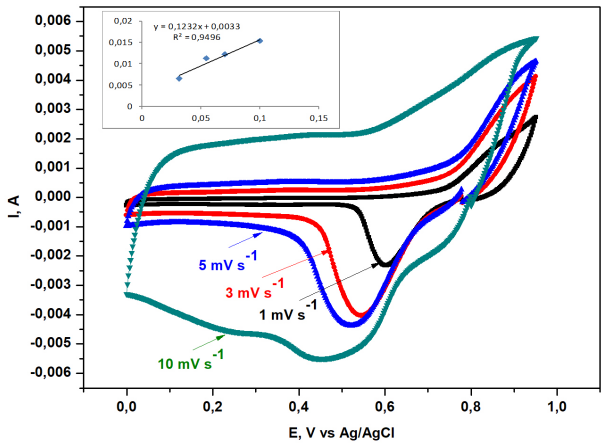


Fig. 5. Cyclic voltammograms on carbon electrode in 0.1 M HCL + 100 mg·L$^{-1}$ $HAuCl_4$ of various scan rates: 1, 3, 5 and 10 mV·s$^{-1}$.

This indicates the catalytic effect of this electrode, which has a reducing property and has a more negative stationary potential (system consisting of $H^+$ | activated carbon) than the system consisting of $AuCl_4^-$ | Au, which is given above.

The scanning electron microscopic images of the gold adsorbed carbon surface was carried out to see the existence of the gold particles and their morphology. SEM images of the carbon electrode surface after deposition are represented in Fig. 6.

In the SEM images, it is clearly seen that the carbon surface is irregular in nature and gold was grown not as a uniform thin film, but as a spherical and prolate (elongated). The smallest gold nanoparticles that could be examined were 100–250 nm in diameter on the surface of the carbon electrode. Submicron gold particles mostly were not grown separately. They are agglomerated and cannot

(a)

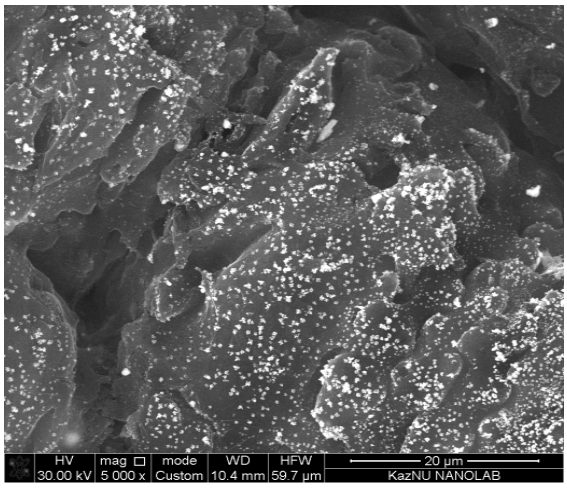


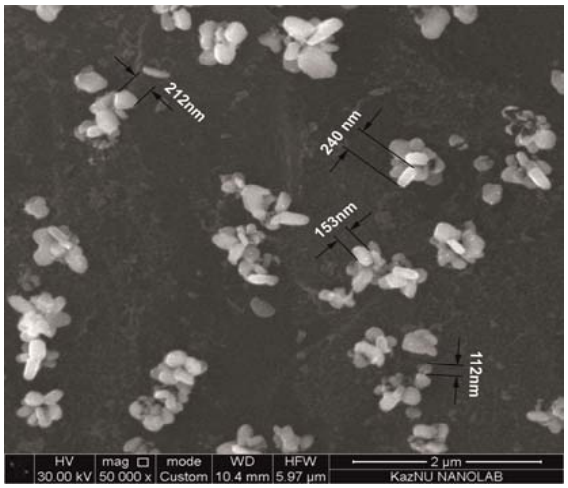


(b)

(c)

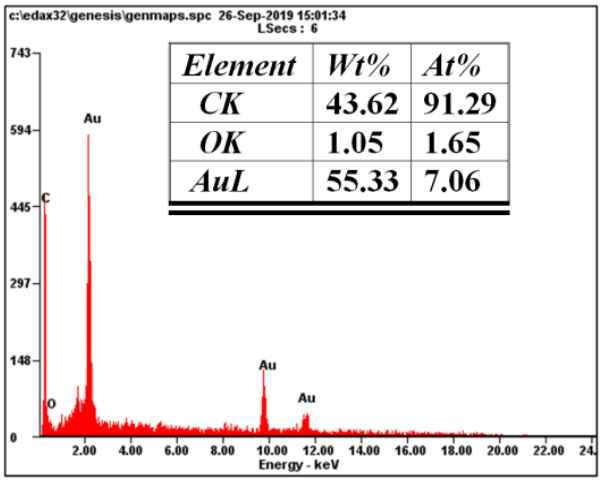


Fig. 6. SEM images at different magnifications (a, b) and elemental analysis (c) of the carbon electrode surface after deposition of gold.

be seen as separate particles in the microimages (Fig. 6a,b). It is still an open question of why they are agglomerated. Elemental analysis by Energy Dispersive X-ray Analysis was carried out to verify the fact that those bright particles are gold (Fig. 6c). Using this method, it is possible to obtain gold nano- and submicron particles and gold can be extracted (recovered) from production waste.

## 4. Conclusions

Within the framework of this work, the electroreduction of $Au^{3+}$ ions on activated carbon and gold electrodes was investigated. Using the piezoquartz microbalance method in combination with voltammetry, the number of electrons participating in the reaction were determined. It was also found that electroreduction of gold goes via the discharge of $AuCl_4^-$ complexes to the formation of metallic gold with a current efficiency of 97–99%. Cyclic voltammograms of both electrodes revealed a linear dependence of $j_{pc}$ vs. $v^{1/2}$ at the studied scan rates of 1–50 $mV \cdot s^{-1}$, which indicates the diffusion limitation of the electrochemical reduction of gold. Based on the Rends-Ševčik equation, the diffusion coefficient of $Au^{3+}$ ions was calculated. Diffusion coefficient of $Au^{3+}$ ions for the concentration of 100 $mg \cdot L^{-1}$ on gold and carbon electrodes is determined by the CV method and the values of the coefficient are $1.6 \cdot 10^{-5}$ $cm^2 \cdot s^{-1}$ and 56.0 $cm^2 \cdot s^{-1} \cdot g^{-1}$, respectively. It was also revealed that electroreduction of gold on an activated carbon electrode comes with a high limiting cathode current compared to a gold electrode which is caused by a high specific surface area of the material. When i = 0, the system measured at a constant open circuit potential of about +420 mV vs. Ag/AgCl.

## Acknowledgments

The work was carried out in the framework of project No. AP05134691 by the support of the Ministry of Education and Science of the Republic of Kazakhstan.

## References


[1]. E.J. Calvo, R.A. Etchenique, *Comprehensive Chemical Kinetics* 37 (1999) 461–487. DOI: 10.1016/S0069-8040(99)80017-X

[2]. R. Chauhan, J. Singh, P.R. Solanki, T. Manaka, M. Iwamoto, T. Basu, B.D. Malhotra, *Sensor. Actuat. B-Chem.* 222 (2016) 804–814. DOI: 10.1016/j.snb.2015.08.117

[3]. G. Sauerbrey, *Z. Phys.* 155 (1959) 206–222. DOI: 10.1007/BF01337937

[4]. E. Gileadi, V. Tsionsky, *J. Electrochem. Soc.* 147 (2000) 567–574. DOI: 10.1149/1.1393234

[5]. Thiago R.L.C. Paixão, Eduardo A. Ponzio, Roberto M. Torresi, Mauro Bertotti, *J. Braz. Chem. Soc.* 17 (2006) 374–381. DOI: 10.1590/S0103-50532006000200023

[6]. V.G. Celante, M.B.J.G. Freitas, *J. Appl. Electrochem.* 40 (2010) 233–239. DOI: 10.1007/s10800-009-9996-x

[7]. V. Pavlenko, Zh. Supiyeva, Q. Abbas, T. Kon'kova, N. Abeykoon, N. Prikhodko, M. Bijsenbayev, A. Kurbatov, Z. Mansurov, *Eurasian Chem. Tech. J.* 20 (2018) 99–105. DOI: 10.18321/ectj695

[8]. S. Azat, R. Busquets, V. Pavlenko, A. Kerimkulova, R. Whitby, Z. Mansurov, *Applied Mechanics and Materials* 467 (2014) 49–51. DOI: 10.4028/www.scientific.net/AMM.467.49

[9]. V. Pavlenko, S. Azat, A. Kerimkulova, Z. Mansurov, *Advanced Materials Research* 535–537 (2012) 1041–1045. DOI: 10.4028/www.scientific.net/AMR.535-537.1041

[10]. A. Atchabarova, R. Tokpayev, A. Kabulov, S. Nechipurenko, R. Nurmanova, S. Yefremov, M. Nauryzbayev, *Eurasian Chem. Tech. J.* 2 (2016) 141–147. DOI: 10.18321/ectj440

[11]. P.A. Schmitz, S. Duyvesteyn, W.P. Johnson, L. Enloe, J. McMullen, *Hydrometallurgy* 61 (2001) 121–135. DOI: 10.1016/S0304-386X(01)00164-5

[12]. E.J. Bain, J.M. Calo, R. Spitz-Steinberg, J. Kirchner, J. Axen, *Energ. Fuel.* 24 (2010) 3415–3421. DOI: 10.1021/ef901542q

[13]. H.M. Albishri, H.M. Marwani, *Arab. J. Chem.* 9 (2016) S252–S258. DOI: 10.1016/j.arabjc.2011.03.017

[14]. Ş. Parlayıcı, E. Pehlivan, *International Proceedings of Chemical, Biological and Environmental Engineering* 101 (2017) 142–148.

[15]. Z.A. Mansurov, Carbon nanostructured materials based on plant raw materials, Kazakh National University, Almaty, 2010, 301 p.

[16]. R.M. Mansurova, V.A. Zakharov, I.M. Bessarabova, N.K. Zhylybayeva, Z.A. Mansurov, *Eurasian Chem. Tech. J.* 6 (2004) 255–265.

[17]. V.A. Zakharov, I.M. Bessarabova, R.M. Mansurova, A.F. Nikolaeva, *Chemical Bulletin of Kazakh National University* 3 (2003) 129–135.

[18]. Zh. Supiyeva, Kh. Avchukir, V. Pavlenko, M. Yeleuov, A. Taurbekov, G. Smagulova, Z. Mansurov, *Materials Today: Proceedings*, DOI: 10.1016/j.matpr.2019.11.013